



ISTITUTO NAZIONALE DI RICERCA METROLOGICA Repository Istituzionale

Validation of the sensitivity analysis method of coordinate measurement uncertainty evaluation

Original

Validation of the sensitivity analysis method of coordinate measurement uncertainty evaluation / Wojtyła, Mirosław; Rosner, Paweł; Płowucha, Wojciech; Forbes, Alistair B.; Savio, Enrico; Balsamo, Alessandro. - In: MEASUREMENT. - ISSN 0263-2241. - 199:(2022), p. 111454. [10.1016/j.measurement.2022.111454]

Availability:

This version is available at: 11696/74420 since: 2022-06-15T15:10:22Z

Publisher:

Elsevier

Published

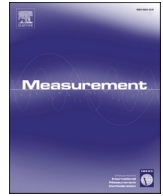
DOI:10.1016/j.measurement.2022.111454

Terms of use:

This article is made available under terms and conditions as specified in the corresponding bibliographic description in the repository

Publisher copyright

(Article begins on next page)



Validation of the sensitivity analysis method of coordinate measurement uncertainty evaluation

Mirosław Wojtyła^{a,*}, Paweł Rosner^a, Wojciech Płowucha^a, Alistair B. Forbes^b, Enrico Savio^c, Alessandro Balsamo^d

^a University of Bielsko-Biala (Laboratory of Metrology), Bielsko-Biala, Poland

^b National Physical Laboratory, Teddington, UK

^c University of Padova (Department of Industrial Engineering), Padova, Italy

^d INRIM (National Institute of Research in Metrology), Torino, Italy

ARTICLE INFO

Keywords:

Coordinate measuring machines (CMM)
Measurement uncertainty
Geometrical product specification (GPS)
Sensitivity analysis
GUM uncertainty framework (GUF)

ABSTRACT

The paper presents the results of the tests carried out to validate a new method for evaluating the uncertainty of coordinate measurements categorised as the Sensitivity Analysis (SA). This method concerns measuring dimensions and geometrical deviations. Measurement uncertainty is evaluated on the basis of information given in the Maximum Permissible Error (MPE) formula for a Coordinate Measuring Machine (CMM). Measurement models express the measured characteristics as a function of differences of coordinates of a small number of appropriately selected points of the workpiece. If reverification test results for the CMM used are available, then the estimated uncertainty takes into account the actual accuracy of the CMM. General formulae are given to calculate the uncertainty of measurement of a circle diameter and coaxiality. The relevant experiment is based on ISO 15530-3 recommendations. A calibrated cylindrical square was used for validation. 17 circles' diameters and 84 different combinations of datum length and distance of the toleranced element from the datum for measuring coaxiality were adopted as validated characteristics. The validation results are presented in tables and graphs and the chi-square test for equality of variances was used to confirm that the method is correct. The validation results are positive.

1. Introduction

Since the publication of the “Guide to the expression of uncertainty in measurement” (GUM) [1], there is no need to justify that measurement uncertainty is an important component of the measurement result. Documents [2] and [3] point out that the information contained in the measurement uncertainty has an important practical (and even economic) aspect. As a certain simplification, it can be said that for this reason, the document [4] requires knowledge of the uncertainties of measurements carried out in the automotive industry.

Coordinate measurements have been the basic technique used in product control and quality control in the machine industry and, especially, in the automotive and aerospace industries for many years. The topic of uncertainty evaluation of coordinate measurements has a long history. Already in 2001, in the publication [5], by using the term “task-specific uncertainty”, attention is drawn to the specificity of coordinate

measurements, namely that the various characteristics (dimensions, geometrical deviations) [6,7] are measured with various uncertainties. Attention is drawn to the large number of factors affecting the accuracy of the coordinate measurement. Methods for evaluating uncertainty are mentioned, such as sensitivity analysis, expert judgements, experimental method using calibrated objects, statistical estimations from measurement and computer calculations (virtual CMM, simulation by constraints). References contain 124 entries. Both this and other publications and documents (e.g., also GUM [1] and EA-4/02 [8]) use terms such as Type A and Type B evaluations (distinguishing that information about uncertainty components has been obtained experimentally or otherwise), *a priori* and *a posteriori* methods (uncertainty evaluated already before or after measurements), or finally, “analytical methods”, “GUM uncertainty framework (GUF)” and “Monte Carlo method (MCM)” as the methods of propagation of the uncertainty components.

The standardization work carried out by ISO TC 213 resulted in ISO

* Corresponding author.

E-mail addresses: mwojtyla@ath.bielsko.pl (M. Wojtyła), lm@ath.bielsko.pl (P. Rosner), wplowucha@ath.bielsko.pl (W. Płowucha), alistair.forbes@npl.co.uk (A.B. Forbes), enrico.savio@unipd.it (E. Savio), a.balsamo@inrim.it (A. Balsamo).

<https://doi.org/10.1016/j.measurement.2022.111454>

Received 21 March 2022; Received in revised form 24 May 2022; Accepted 7 June 2022

Available online 10 June 2022

0263-2241/© 2022 The Author(s). Published by Elsevier Ltd. This is an open access article under the CC BY-NC-ND license (<http://creativecommons.org/licenses/by-nc-nd/4.0/>).

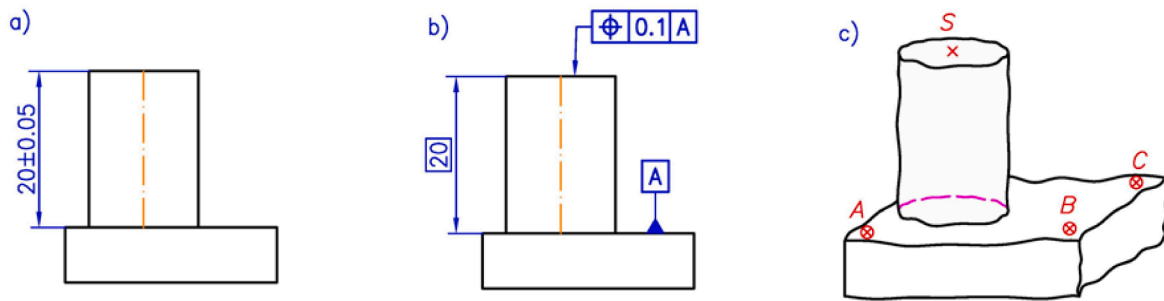


Fig. 1. Example explaining the essence of the SA method: a) pin length (as tolerated dimension), b) top plane position related to datum plane A, c) essential points arrangement.

15530-3:2011 [9] and two technical specifications: ISO/TS 15530-1:2013 [10] and ISO/TS 15530-4:2008 [11]. Technical specification [10] outlines three techniques for evaluating the uncertainty in coordinate measurements: “use of calibrated workpieces or standards”, “simulation” and “sensitivity analysis”. The term: “use of multiple measurement strategies in measurements of artefacts”, also appears in the literature. In [12], one of the uncertainty determination techniques is called “using uncertainty budget”. At the same time, some metrology institutes use software called “Virtual CMM (VCMM)”, which is supplied by PTB [13,14]. Many centres indicate that they use proprietary uncertainty analysis techniques for measuring tasks performed on CMM [15–18] (to mention only a few of many listed ones).

The method described in ISO 15530-3 [9] can be regarded as a reference method, meaning that it does not require validation. Other methods for evaluating uncertainty should be validated, in particular because they use different simplifying assumptions. The need for validation is noted in ISO/TS 15530-4 [11], in particular with regard to simulation software, but it may be deemed to refer also to any “uncertainty evaluation software (UES)”.

We still lack a simple, easy-to-use and easy-to-understand technique for evaluating the uncertainty of coordinate measurements. Between 2019 and 2022, three new methods for evaluating the uncertainty: one *a posteriori* method and two *a priori* methods, were investigated as part of the EUCoM project [19]. In this paper, we will focus on the problem of validation of one of the *a priori* methods. The method was developed at University of Bielsko Biala (ATH) and is called “sensitivity analysis (SA) method”. A lot of information about this method has already been published, e.g. in [20,21]. Two important components of this method, namely the developing of the measurement model and the proposal for the use of information contained in the acceptance and reverification test results for the CMM used, will be briefly recalled. The results of validation studies are the key content of this paper.

In this paper, the uncertainty evaluated by the technique described in [9] is called “experimental uncertainty” and the validated method is called “SA method”.

2. Basic assumptions of the “SA method”

In coordinate metrology, geometrical elements such as planes and cylinders are the basic components of any measured object. These elements can be combined to create more complex measured values (characteristics). For example, an object consists of a pin nominally perpendicular to a flat plate and the characteristic measured is the distance between the top surface of the pin and the surface of the plate (Fig. 1a) or the position of top plane (Fig. 1b).

The measured characteristics are related to two elements: the surface of the plate and the top surface of the pin. In coordinate measurements, the probing points on both elements are associated (association - feature operation used to fit ideal feature(s) to non-ideal feature(s) according to a criterion, see ([22], (3.4.1.4)) to the ideal elements, which gives two planes in this case. The measured characteristic is distance between the

lower and the upper planes (Fig. 1a) or the position of the upper plane related to the datum plane A (Fig. 1b).

One of the difficulties in evaluating the uncertainty of such measurements is the lack of a compact expression for associating the ideal elements with the probing points through the best fit. This makes it difficult to apply the primary GUF concept, in which the first step is to define the measurement model.

In order to overcome this problem, the new method for evaluation uncertainty (SA method) brought the number of points to a minimum, relevant from the point of view of the form (size and shape) of the object and the measured characteristics. These important points are not necessarily taken from those really probed, but rather are artificially selected points representing the object and the measured characteristics. In the above example of a pin and a flat plate, the representative points are three points on the bottom surface and only one on the top surface of the pin. The measured value is then the distance between the point on the top surface, S, and the plane containing three points, A, B, C. The number of significant points is minimal, there is no matching problem and the measured value can be expressed in a compact form as a function of the coordinates of these significant points. This is an effective measurement model and allows conventional uncertainty assessment according to the GUF by deriving sensitivity factors. In general, these points may lie on the integral feature (plane, cylinder, etc.) or on the derived feature (e.g., cylinder or cone axes). An example of a model where all (three) points lie on the axis of a cylinder/cylinders is the coaxiality model used in this paper.

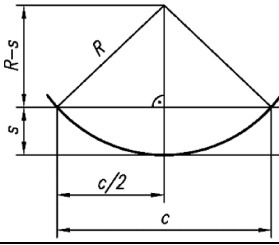
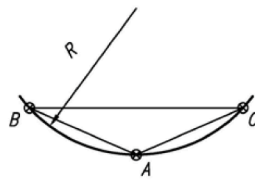
The exact position of key points is not directly associated with the probing strategy. They shall be taken where relevant to the nature of the workpiece and in a reasonable manner consistent with the dimensions and possible obstacles. In this example, the three key points on a flat surface will be spaced as far as possible due to the dimensions of the plate and the pin.

A loose relationship with the actual or planned probing strategy is the main approximation on which the SA method is based. There is no effect of point redundancy or of the actual positions of individual points. The description of the method also ignores the fact that the significant points adopted on the derived feature result from a certain number of probing points for that feature. A key element of this method is that a small number of well-chosen significant points is indeed sufficient for an approximate but easy assessment of uncertainty.

The basic information resulting from the measurements is the distance between the pairs of points. The value measured in the above example is clearly the distance, but it can be expressed as the position of the face of the pin when the bottom plane is regarded as the datum (Fig. 1b). The distances can be broken down into the differences of coordinates of particular points. Finally, the measured value can be expressed as a function of differences of coordinates of the significant points.

The model from Fig. 1 is to show that the SA method applies to any geometric characteristic, in particular to all geometric deviations occurring in the ISO 1101 and to show an important element of the SA

Table 1
Theoretical basis of the SA method.

<p>Classical microscope measurement</p> <p>Principle of measuring the arc radius with a microscope</p> 	<p>Coordinate measurement (2D case)</p> <p>Principle of measuring the radius coordinates</p> 																																																												
<p>The measured values are the sagitta s and the chord c</p>	<p>The measured values are the coordinates of points $A(x_A, y_A), B(x_B, y_B), C(x_C, y_C)$</p>																																																												
<p>The radius R of the arc is calculated as follows</p> $R(c, s) = \frac{c^2}{8s} + \frac{s}{2}$ <p>where: c - chord length, s - sagitta length</p>	<p>The radius R of the circle is calculated as follows:</p> $R = \frac{abc}{4P}$ <p>where: a, b, c – the length of the sides of the triangle; P – the triangle area. The length of the sides a, b, c and area P are expressed as differences in the coordinates of points A, B, C: $a = \sqrt{x_{BC}^2 + y_{BC}^2}$, etc.</p>																																																												
<p>Input quantities for models</p> <p>Chord and sagitta lengths c, s</p>	<p>Coordinate differences $x_{AB}, y_{AB}, x_{AC}, y_{AC}, x_{BC}, y_{BC}$ where $x_{AB} = x_B - x_A$, etc.</p>																																																												
<p>Uncertainty budget (see equations (1) - (4)). Example for $R = 40$ mm, $s = 15$ mm, $E_{L,MPE} = \pm(4 + 6L/1000)$, μm, $b = 0,577$</p>																																																													
<table border="1"> <thead> <tr> <th></th> <th>x_i, mm</th> <th>$\frac{\partial R}{\partial x_i}$</th> <th>$u_{xi}$, μm</th> <th>$\frac{\partial R}{\partial x_i} u_{xi}$, μm</th> </tr> </thead> <tbody> <tr> <td>s</td> <td>15.000</td> <td>-1.667</td> <td>2.361</td> <td>-3.935</td> </tr> <tr> <td>c</td> <td>62.450</td> <td>1.041</td> <td>2.526</td> <td>2.629</td> </tr> <tr> <td></td> <td></td> <td></td> <td>u</td> <td>4.732</td> </tr> </tbody> </table>		x_i , mm	$\frac{\partial R}{\partial x_i}$	u_{xi} , μm	$\frac{\partial R}{\partial x_i} u_{xi}$, μm	s	15.000	-1.667	2.361	-3.935	c	62.450	1.041	2.526	2.629				u	4.732	<table border="1"> <thead> <tr> <th></th> <th>x_i, mm</th> <th>$\frac{\partial R}{\partial x_i}$</th> <th>$u_{xi}$, μm</th> <th>$\frac{\partial R}{\partial x_i} u_{xi}$, μm</th> </tr> </thead> <tbody> <tr> <td>x_{AB}</td> <td>31.225</td> <td>0.400</td> <td>2.418</td> <td>0.968</td> </tr> <tr> <td>y_{AB}</td> <td>15.0</td> <td>0.833</td> <td>2.361</td> <td>1.968</td> </tr> <tr> <td>x_{AC}</td> <td>31.225</td> <td>0.400</td> <td>2.418</td> <td>0.968</td> </tr> <tr> <td>y_{AC}</td> <td>15.0</td> <td>0.833</td> <td>2.361</td> <td>1.968</td> </tr> <tr> <td>x_{BC}</td> <td>62.450</td> <td>0.641</td> <td>2.526</td> <td>1.618</td> </tr> <tr> <td>y_{BC}</td> <td>0.0</td> <td>0.000</td> <td>2.309</td> <td>0.000</td> </tr> <tr> <td></td> <td></td> <td></td> <td>u</td> <td>3.498</td> </tr> </tbody> </table>		x_i , mm	$\frac{\partial R}{\partial x_i}$	u_{xi} , μm	$\frac{\partial R}{\partial x_i} u_{xi}$, μm	x_{AB}	31.225	0.400	2.418	0.968	y_{AB}	15.0	0.833	2.361	1.968	x_{AC}	31.225	0.400	2.418	0.968	y_{AC}	15.0	0.833	2.361	1.968	x_{BC}	62.450	0.641	2.526	1.618	y_{BC}	0.0	0.000	2.309	0.000				u	3.498
	x_i , mm	$\frac{\partial R}{\partial x_i}$	u_{xi} , μm	$\frac{\partial R}{\partial x_i} u_{xi}$, μm																																																									
s	15.000	-1.667	2.361	-3.935																																																									
c	62.450	1.041	2.526	2.629																																																									
			u	4.732																																																									
	x_i , mm	$\frac{\partial R}{\partial x_i}$	u_{xi} , μm	$\frac{\partial R}{\partial x_i} u_{xi}$, μm																																																									
x_{AB}	31.225	0.400	2.418	0.968																																																									
y_{AB}	15.0	0.833	2.361	1.968																																																									
x_{AC}	31.225	0.400	2.418	0.968																																																									
y_{AC}	15.0	0.833	2.361	1.968																																																									
x_{BC}	62.450	0.641	2.526	1.618																																																									
y_{BC}	0.0	0.000	2.309	0.000																																																									
			u	3.498																																																									

method, which is to reduce the number of points of individual surfaces to a minimum.

The CMM’s ability to accurately measure distance is specified as the length measurement error, E_L . It is the metrological characteristics of CMM as defined in ISO 10360 [23], available to most CMMs under a metrological confirmation regime. E_L (or $E_{L,MPE}$) is used to determine input uncertainties in the measurement model.

The details of assumptions and the analysis of some models developed for this approach have been published in [20,21]. Their key features are:

- According to the classification of uncertainty evaluation techniques in coordinate metrology, as given in ISO/TS 15530–1 [10], the method presented falls within the sensitivity analysis category.

- The method is in compliance with the GUF [1]. A model has been developed for individual coordinate measurements from which sensitivity factors are derived. Input uncertainties are estimated and converted into combined uncertainty components by multiplying them by sensitivity factors. In other words, the coordinate measurement is treated as an indirect measurement based on the minimum number of points. According to SA method, assuming that there is no correlation, combined measurement uncertainty, u_{SA} , is calculated as follows.

$$u_{SA} = \sqrt{\sum_{i=1}^n \left(\frac{\partial l}{\partial x_i} u_{xi} \right)^2} \tag{1}$$

– Input standard uncertainties u_{xi} are calculated using method B according to the recommendations of ISO 14253–2 ([24], (8.3.2)). The maximum permissible error a is multiplied by the factor b , which takes into account the known/accepted error probability distribution (if uniform, then $b = 1/\sqrt{3}$, if normal, then $b = 1/2$ or even $b = 1/3$):

$$u_{xi} = a \bullet b \tag{2}$$

– Often, the measurement error is mainly caused by a measuring instrument. The standard ([24], (8.4.5)) suggests using the value of the maximum permissible error (MPE) assigned to the instrument. For CMM, the relevant MPE is $E_{L,MPE}$ (ISO 10360–2 [23]):

$$a = E_{L,MPE} \tag{3}$$

which results in

$$u_{xi} = E_{L,MPE} \bullet b \tag{4}$$

– In the absence of other information, as *a priori* probability distribution uniform distribution should be assumed. When the actual results

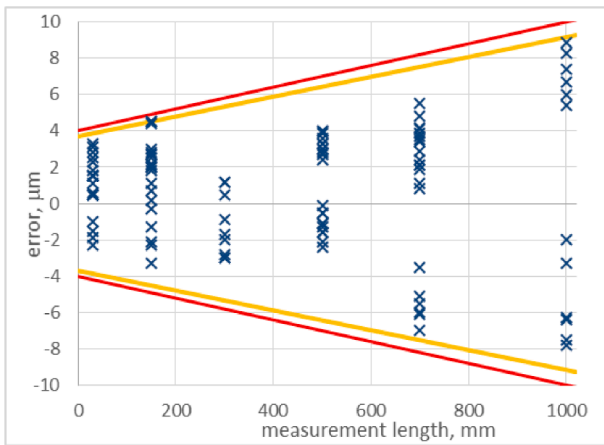


Fig. 2. Reverification test results for CMM Aberlink with $E_{L,MPE} = \pm(4 + 6L/1000) \mu\text{m}$ (outside lines); lines $\pm 2u$ are also shown for b calculated according to equations (5) ($b_2 = 0.459$).

of acceptance test or reverification test for a specific CMM are available, values b can be derived from them. Both possibilities are analysed in this paper.

- The most important feature of the SA method is that the input values in the measurement model are the distances, namely the differences of the coordinates of the points used to define the particular characteristics (dimensions and geometrical deviations).

- The method is described by means of explicit equations and is similar to the cases known from classical geometrical metrology, which can be easily demonstrated by comparing the arc radius measurement with a microscope (using sagitta and chord lengths) with the coordinate measurement [25] (Table 1).

- The model does not take into account the influence of form deviations and the number of probing points. Table 1 serves to show that the proposed method of estimating the uncertainty of coordinate measurements is very similar to the methods previously used in classical measurements and therefore should be understandable.

3. Distance measurement uncertainty

The standard measurement uncertainty u of the distance between two points (or the differences in the coordinates of two points) is assumed to be calculated using formula (2). In the simplest but secure approach, assuming a uniform distribution $b_1 = 1/\sqrt{3} \approx 0.577$. The value b can take into account the actual accuracy of the CMM. The results of the actual acceptance test and reverification test show that errors often represent a small part of the maximum permissible error $E_{L,MPE}$, especially for new CMMs.

In order to take into account the actual accuracy of the CMM, it is proposed that the factor b_2 is assessed as the sample second-order

moment relative to zero ([26], (1.14)) of test results (errors of indications) normalized for the range (-1, 1):

$$b_2 = \sqrt{\frac{1}{N} \sum_{i=1}^N E_{n,L,i}^2} \tag{5}$$

where $N = 105$ (total number of measurements in ISO 10360-2 test) and

$$E_{n,L,i} = \frac{E_{L,i}}{E_{L,MPE,i}} \tag{6}$$

Fig. 2 shows the results of the CMM reverification test used to validate the uncertainty estimation method. The test was performed in accordance with ISO 10360-2, using gauge blocks with lengths of 30, 150, 300, 500, 700 and 1000 mm. In the “measurements” along the individual axes, 5 gauge blocks with a length of up to 700 mm were used. For “measurements” along the diagonals, a 1000 mm gauge block was

Table 2

An example circle diameter measurement uncertainty budget for the following data: $E_{L,MPE} = \pm(4 + 6L/1000) \mu\text{m}$, uniform distribution ($b_1 = 0.577$), $D = 80$ mm; in the measurement model, points A, B and C are evenly spaced (every 120°).

	x_i	$\partial D / \partial x_i$	u_{xi}	$\partial D / \partial x_i \cdot u_{xi}$
x_{AB}	-34.64	0.577	2.43	1.40
y_{AB}	-60.00	-0.333	2.52	-0.84
z_{AB}	0	0	2.31	0
x_{AC}	34.64	-0.577	2.43	-1.40
y_{AC}	-60.00	-0.333	2.52	-0.84
z_{AC}	0	0	2.31	0
x_{CB}	-69.28	-1.155	2.55	-2.94
y_{CB}	0	0	2.31	0
z_{CB}	0	0	2.31	0
			$u_{SA(D)}$	3.74
			$U_{SA(D)}$	7.49

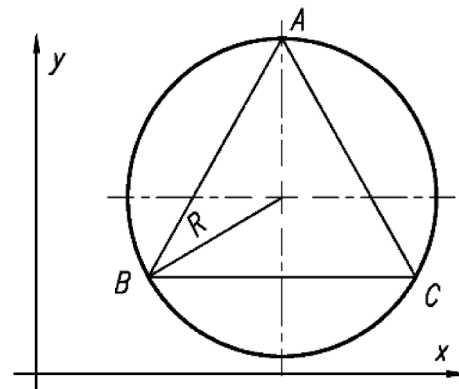


Fig. 4. Positions of points for the circle diameter measurement model.

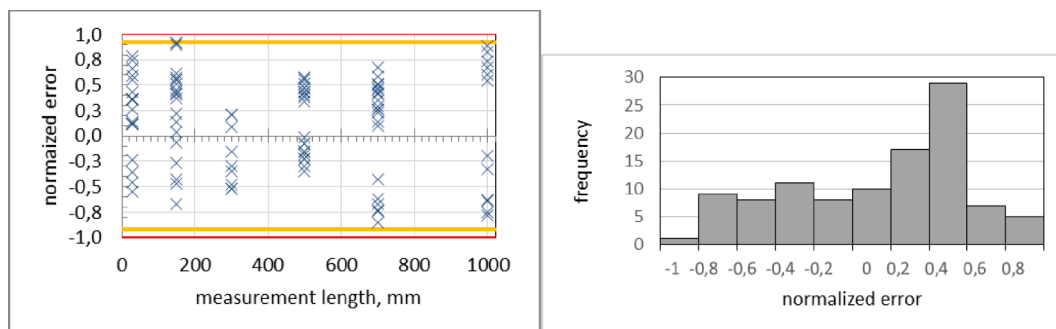


Fig. 3. Normalized measurement errors from reverification test: a) graph with $E_{L,MPE}$ and $\pm 2u$ (equation (5)), b) histogram.

used instead of the 300 mm. Normalization of CMM errors was performed according to the formula (6).

Fig. 3 shows normalized errors of indications and lines corresponding to $\pm 2u$ for b_2 estimated according to the formulae (5–6).

$$u_{SA}(D) \approx 2b \bullet \sqrt{2[0.289 \bullet E_{L,MPE}(0.433D)]^2 + 2[0.167 \bullet E_{L,MPE}(0.75D)]^2 + [0.577 \bullet E_{L,MPE}(0.866D)]^2} \tag{9}$$

The value b_2 calculated by the formula (5) is equal to 0.459, namely slightly less than for the uniform distribution, where $b_1 = 0.577$. Although some asymmetry is visible in Fig. 3, no error value is outside the lines defined by $\pm 2u$.

For validation purposes, the uncertainty u_{SA} evaluated according to the SA method will be calculated for two values of factor b :

- resulting from the assumption of a uniform error distribution for CMM ($b_1 = 0.577$) (u_{SA1}), and.
- resulting from the current accuracy contained in the results of the reverification test, calculated by the formula (5) ($b_2 = 0.459$) (u_{SA2}).

4. Measurement models

According to recommendation contained in ISO/TS 15530–4, the validation of SA method will be performed using the cylindrical square. The diameter of the circle and the coaxiality were assumed as the measured characteristics.

4.1. Circle diameter measurement model

Different formulae are available in the literature to calculate the diameter D of a circle based on knowledge of the coordinates of three points. The simplest one is the formula for the diameter of a circle circumscribed about a triangle:

$$D = \frac{abc}{2P} \tag{7}$$

where P is the area of the triangle, and a, b, c are the lengths of its sides, which can be expressed by the differences of coordinates of the points - the vertices of the triangle. In turn, the area of the triangle P can be expressed by the cross product of the two sides of the triangle:

$$P = \frac{|AB \times AC|}{2} \tag{8}$$

Uncertainty assessment is based on 9 input values (coordinates of **AB**, **AC**, **BC** vectors). Sensitivity factors are derived as partial derivatives, calculated analytically or numerically. An uncertainty budget is shown in Table 2.

In the example, the circle lies in the xy plane. The positions of points A, B, C as shown in Fig. 4.

The budget presented in Table 2 clearly show that the developed method for coordinate measurements is in line with the GUM. The uncertainty components appears in the uncertainty budget with the weight

value equal to 0.577 for x_{CB} , 0.289 for x_{AB} and x_{AC} , and 0.167 for y_{AB} and y_{AC} . Then, general formula for calculating the standard uncertainty $u_S(D)$ of the circle diameter using SA method, can be presented as:

All factors in the formula (9) are derived from the partial derivatives given in Table 2 and from the trigonometric function values associated with the points spaced every 120° .

4.2. Coaxiality measurement model

There are two basic instances of coaxiality tolerance. In the first, the tolerated element (axis of the right cylinder, Fig. 5a) is at a certain distance from the datum which is the axis of the left cylinder. In the latter case, the tolerated element (axis of the central cylinder, Fig. 5b) is located between the two datums A and B which establish the common datum $A-B$ (common axis of the outer cylinders).

Coaxiality is the smallest diameter of the cylinder coaxial with the cylinder which is the datum (represented by points A and B) and containing all the axis points of the tolerated element, represented here by point S [6]. So, it takes into account only two points of the datum A and B and one point of the tolerated element. Coaxiality CX is therefore twice the distance ds of point S from straight line AB :

$$CX = 2 \bullet ds(S, AB) \tag{10}$$

The formula for the distance of point S from straight line AB is ([22], (Table B.7)):

$$ds(S, AB) = \left| BS \times \frac{AB}{|AB|} \right| \tag{11}$$

There are 6 input quantities in the model ($x_{AB}, y_{AB}, z_{AB}, x_{BS}, y_{BS}$ and z_{BS}) generally designated as x_i . An uncertainty budget is shown in

Table 3

Uncertainty budget for coaxiality; $E_{L,MPE} = \pm(4 + 6L/1000)$, μm , uniform distribution ($b_1 = 0.577$), datum length $l = 25$ mm, distance of tolerated element from datum $L = 40$ mm.

	x_i	$\partial ds / \partial x_i$	u_{xi}	$\partial ds / \partial x_i \bullet u_{xi}$
x_{AB}	25	0	2.40	0
y_{AB}	0	0	2.31	0
z_{AB}	0	-1.6	2.31	-3.70
x_{BS}	40	0	2.45	0
y_{BS}	0	0	2.31	0
z_{BS}	0.01	1	2.31	2.31
			$u_{SA}(S-AB)$	4.36
			$u_{SA}(CX)$	8.72
			$U_{SA}(CX)$	17.43

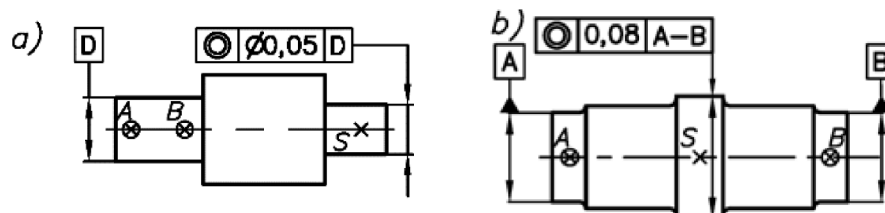


Fig. 5. Two examples of coaxiality specifications; the tolerated element: a) is at a certain distance from the datum, b) is located between the two datums forming the common datum.



Fig. 6. Measurement of the cylinder square.

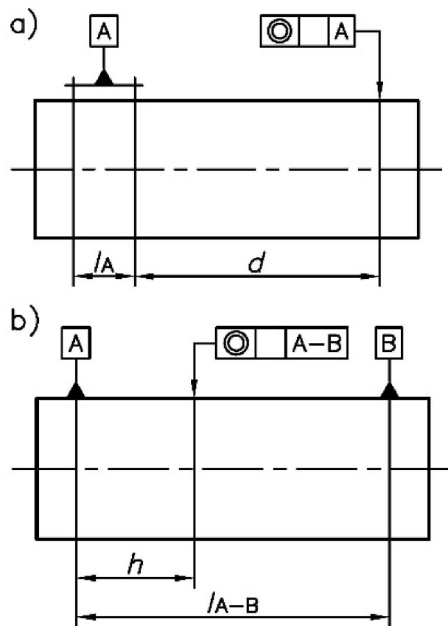


Fig. 7. Drawing of a cylinder with an indication of the datums and toleranced elements for coaxiality: a) a toleranced element outside the datum, b) a toleranced element between the datums (common datum).

Table 3.

The example assumes that the workpiece is oriented along the x -axis. The difference in coordinates x of points A and B is indicated as x_{AB} and the difference in coordinates of points B and S is indicated as z_{BS} (the S point is assumed to be in the xz plane at a short distance from the datum axis). Uncertainties of only two (from six) input values (z_{AB} and z_{BS}) are not zero.

The uncertainty components for z_{BS} and z_{AB} occur in the uncertainty budget with weights 1 and x_{BS}/x_{AB} respectively (in example $x_{BS}/x_{AB} = 1.6$). Therefore, the general equation for the standard uncertainty of the measurement of coaxiality is:

$$u_{SA}(CX) = 2\sqrt{1^2 + \left(\frac{L}{l}\right)^2} \cdot E_{L,MPE}(0) \cdot b \quad (12)$$

where L is the distance of the toleranced element from the datum ($|$

Table 4

Summary of the experiment plan for coaxiality.

Symbol	Dimension	Values	Description
l_A	Datum length (A) (left-most extreme part of cylinder)	(10, 15, 20, 25, 30, 35) mm	
l_{A-B}	Distance between two datums (A-B)	80 mm	
d	Distance of the toleranced element from the datum (A)	(5, 10, 15, 20, 25, 30, 35, 40, 45, 50, 55, 60, 65, 70) mm	The smallest length of the datum $l_A = 10$ mm. For longer datums, the number of toleranced element positions decreases (to fit in the length of the cylinder)
h	Distance of the toleranced element from the closer datum from among A and B	(5, 10, 15, 20, 25, 30, 35, 40) mm	Only in the case of the common datum A-B;
U	Expanded measurement uncertainty	U_1, U_2, U_{4W}, U_{4R} U_{SA1}, U_{SA2}	obtained experimentally obtained using SA method
b	Factor b to calculate the standard uncertainty using SA method with $E_{L,MPE}$	$b_1 = 1/\sqrt{3} \approx 0.577$ $b_2 = 0.459$	(b_1) uniform distribution (b_2) comes from reverification test according to ISO 10360-2; equation (5)

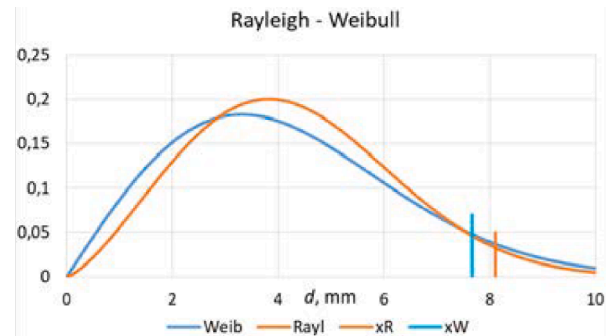


Fig. 8. Example of PDF charts of the Weibull and Rayleigh distributions (matched to the same data) with marked 0.95 quantiles.

$BS]$, l is the length of the datum ($|AB|$), $E_{L,MPE}(0)$ is the maximum permissible measurement error for zero length. When the toleranced element lies outside the datum, the quotient L/l may be (and is usually) significantly greater than 1 (this fact was used to obtain a large range of measurement uncertainty in validation); when it is between datums A and B , that quotient is not greater than 0.5.

5. Validation

5.1. Experiment

Two characteristics, for which the measurement strategy has a significant impact on the uncertainty: the circle diameter and the coaxiality, were selected for the validation of the SA method. In both cases, the experiment consisted in a 20-fold measurement of a calibrated artefact with a known value of the characteristics. Measurements were performed using the Aberlink CMM - Zenith Too with the PH10T measuring head and Aberlink 3D software. The CMM accuracy is expressed by the specification $E_{L,MPE} = \pm(4 + 6L/1000) \mu\text{m}$. The measurements were repeated at longer intervals according to the

Table 5

Comparison of the uncertainties assessed experimentally and using the SA method: hypotheses and critical values for the chi-square test; σ and σ_{SA} are the standard uncertainties evaluated experimentally and using the SA method, respectively.

Test	Null hypothesis H_0	Alternative hypothesis H_1	Null hypothesis criterion
Two-tailed	$\sigma^2 = \sigma_0^2$	$\sigma^2 \neq \sigma_0^2$	$\chi_{cr1}^2 \leq \chi^2 \leq \chi_{cr2}^2$ (0.025, 19) = 8.907, χ_{cr1}^2 (0.975, 19) = 32.852

Table 6

Colours to encode chi-square test results.

Colour	Criterion	Results obtained using the SA method are...
yellow	$\chi^2 < \chi_{cr1}^2$... overestimated
green	$\chi_{cr1}^2 \leq \chi^2 \leq \chi_{cr2}^2$... correct
red	$\chi^2 > \chi_{cr2}^2$... underestimated

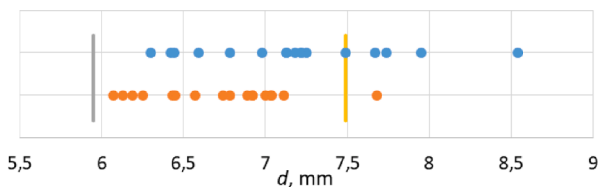


Fig. 9. Outside diameter. Comparison of experimentally determined uncertainty and the SA method.

Table 7

The chi-square test to compare the experimental uncertainties U_1 and U_2 with the uncertainties evaluated using the SA method: $U_{SA1} = 7.49$, $U_{SA2} = 5.95$; $D = 80$ mm (the values of bs and u_p are also given). The test results are colour-coded (see Table 6).

	$bs, \mu\text{m}$	$u_p, \mu\text{m}$	$U_1, \mu\text{m}$	$\chi_1^2(b_1)$	$\chi_2^2(b_2)$	$U_2, \mu\text{m}$	$\chi_1^2(b_1)$	$\chi_2^2(b_2)$
1	0,69	2,80	6,78	16,43	26,00	6,25	13,94	22,05
2	1,27	2,97	7,67	21,02	33,25	6,89	16,94	26,80
3	0,22	3,28	7,22	18,58	29,40	7,00	17,52	27,71
4	0,56	3,12	7,25	18,76	29,68	6,78	16,42	25,98
5	0,52	3,10	7,18	18,39	29,09	6,74	16,21	25,64
6	0,71	2,90	6,98	17,39	27,51	6,43	14,75	23,34
7	0,25	2,84	6,42	14,72	23,29	6,19	13,67	21,63
8	0,18	2,81	6,30	14,15	22,39	6,13	13,40	21,20
9	0,10	3,31	7,13	18,14	28,70	7,04	17,67	27,96
10	0,15	2,99	6,59	15,50	24,53	6,45	14,86	23,51
11	0,44	2,75	6,44	14,81	23,44	6,07	13,13	20,78
12	0,22	3,24	7,13	18,14	28,71	6,92	17,09	27,04
13	-0,55	3,26	7,49	20,00	31,65	7,03	17,62	27,88
14	-0,90	2,92	7,22	18,62	29,45	6,57	15,42	24,40
15	-1,57	2,84	7,74	21,37	33,80	6,92	17,09	27,05
16	-1,37	3,38	8,54	26,05	41,22	7,68	21,05	33,31
17	-1,47	3,01	7,95	22,56	35,69	7,11	18,07	28,59

recommendations in ISO 15530-3 [9]. A cylinder square with a nominal diameter of 80 mm (Fig. 6) was used for the tests.

The diameters and centre coordinates were measured for 17 circles at 5 mm distances, covering 80 mm of the cylinder length. The results were obtained directly for 17 diameters.

From the coordinates of the circle centres, coaxiality was calculated for 7 different datum length and different distances of the tolerated element from the datum. The calculations were performed for six datum lengths of 10, 15, 20, 25, 30, 35 mm (Fig. 7a). Separate calculations were made for the common datum A-B based on two extreme cross-sections (Fig. 7b).

For the case in Fig. 7a, the coaxiality was calculated using the extreme left point of the axis and one of the following points as the datum and one point from the cross-section on the right-hand side of the datum, doing so at ever greater distances from it. This resulted in a total of 69 different combinations of the datum lengths and the distances of

the tolerated element from the datum. For the common datum in Fig. 7b, the points from the two extreme cross-sections were used to define that datum and the coaxiality calculation was performed for 15 points from the other cross-sections.

The experiment plan for coaxiality is summarized in Table 4.

5.2. Experimental uncertainty

In the experimental determination of the measurement uncertainty, the standard [9] requires to correct the bias bs (the symbol bs was introduced to distinguish it from the previously used b denoting a coefficient depending on the type of distribution), and then to estimate the uncertainty as:

$$U = 2 \bullet \sqrt{u_{cal}^2 + u_p^2 + u_{bs}^2 + u_w^2} \tag{13}$$

where

u_{cal} standard uncertainty stated in the calibration certificate of the calibrated workpiece;

u_p standard deviation of results of experiment;

u_{bs} standard uncertainty associated with the corrected systematic error;

u_w standard uncertainty associated with material and manufacturing variations.

As the reference object is made of steel, it has small form deviations and low surface roughness, therefore it was assumed that $u_w = 0$.

Since correction for the systematic error is not possible, three other options were adopted as an alternative.

$$U_1 = 2 \bullet \sqrt{u_{cal}^2 + u_p^2} + |bs| \tag{14}$$

$$U_2 = 2 \bullet \sqrt{u_{cal}^2 + u_p^2 + bs^2} \tag{15}$$

$$U_3 = 2 \bullet \sqrt{u_{cal}^2 + u_{p0}^2} \text{ with } u_{p0} = \sqrt{\frac{\sum_{i=1}^n (y_i - x_{cal})^2}{n - 1}} \tag{16}$$

The formula for U_1 is derived from ISO/TS 15530-3 [27]. According to some authors [28] formula (14) is inconsistent with GUM. The formula for U_2 results from the adoption of the bimodal distribution [12] for bs (in [28] the derivation of the formula (15) is given). In the formula for U_3 , bias is included in u_p (u_p is indicated as u_{p0} to avoid confusion). u_{p0} is calculated as the root of the second-order moment relative to the known value x_{cal} (instead of the mean value \bar{y}). Please note that the second and third equations produce practically identical results ($U_2 \approx U_3$) and only U_2 will be used in subsequent analyses.

These equations are suitable for errors distributed on both sides of the zero, which occurs for characteristics such as dimensions and signed distances.

In the case of errors taking only non-negative values, such as nominally zero distances without a sign (valid in many geometrical specifications), it seems more appropriate to calculate the expanded uncertainty U as 95% of the appropriate distribution quantile ($U = F^{-1}(0.95)$, where F is the cumulative distribution function). The Weibull and Rayleigh distributions are suitable (the Rayleigh distribution is characterized by the distribution of the length of a vector in a plane, the components of which are independent variables with the normal distribution). This gives the next option (for coaxiality):

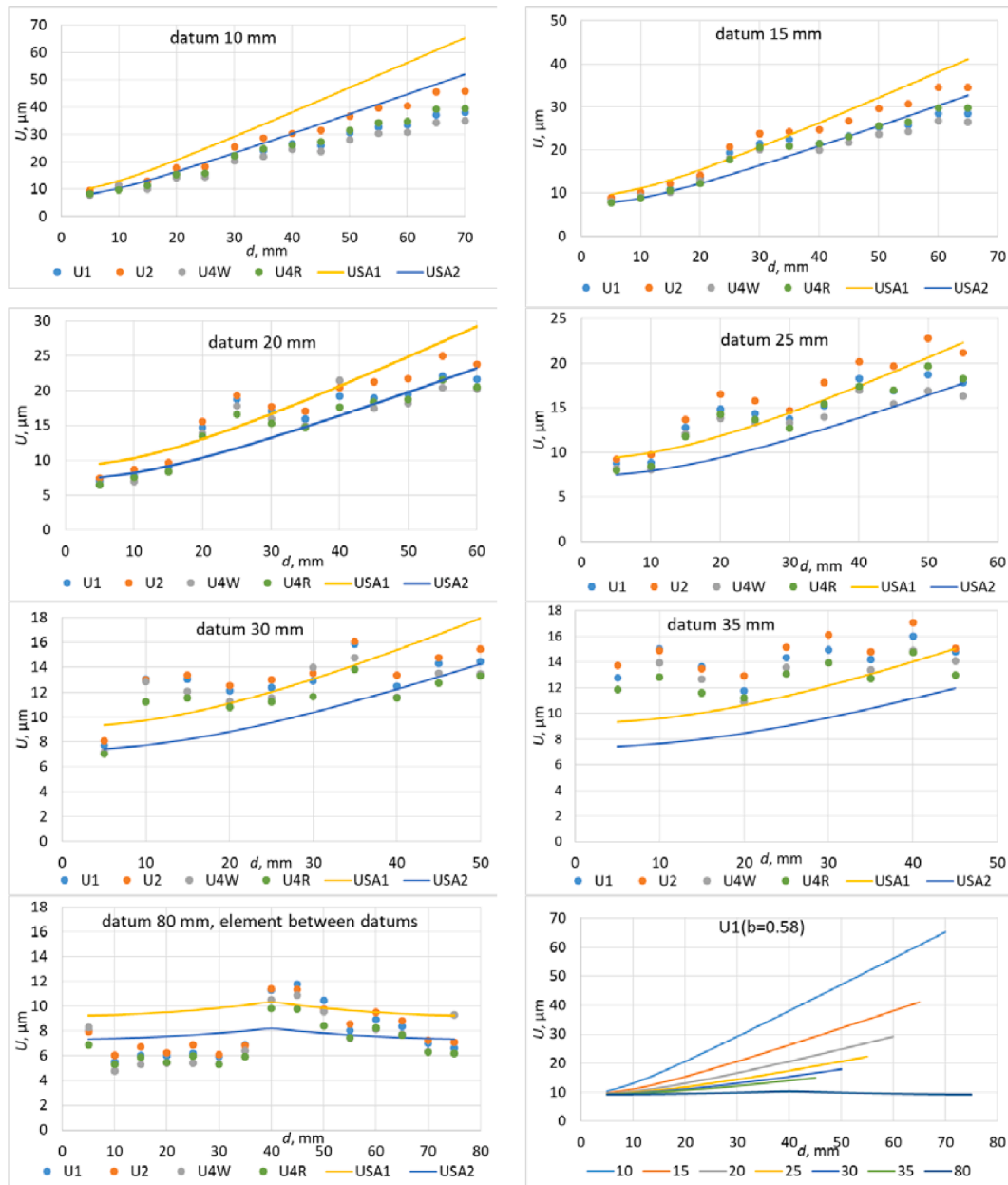


Fig. 10. Graphs of expanded uncertainty values for 6 different lengths of the datum l_A (10–35 mm) and the common datum l_{A-B} (80 mm). The last graph shows all the 7 graphs for U_{SA1} .

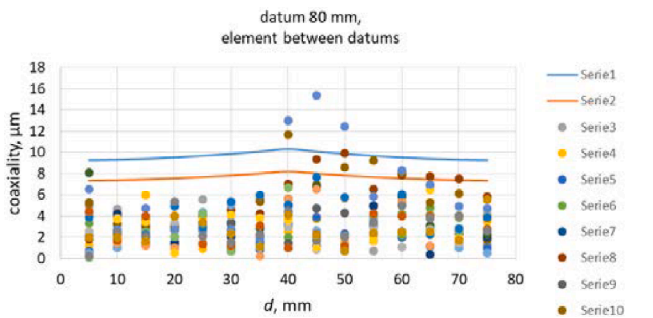


Fig. 11. Summary of the error and uncertainty values determined using the SA method for the “element between datums” case; 5 error values (out of 300) exceed U_{SA1} and 14 exceed U_{SA2} .

$$U_4 = 2 \cdot \sqrt{\left(\frac{F^{-1}(0,95)}{2}\right)^2 + u_{cal}^2} \quad (17)$$

Both of these distributions will be used. For the purpose of distinction, U_4 calculated for the Weibull and Rayleigh distributions are marked U_{4W} and U_{4R} respectively. An example PDF charts of the Rayleigh and Weibull distributions that match the same data are shown in Fig. 8.

Thus, four expanded uncertainty values will be used in further analyses: U_1 , U_2 , U_{4W} and U_{4R} .

5.3. Elaboration of the results – Chi-Square test

The experimentally determined uncertainties evaluated in accordance with [9] were compared to the uncertainties evaluated using the SA method. The chi-square test was conducted for the equality of uncertainties calculated using the SA method and the experimental

Table 8

Chi-square test results for coaxiality (datum length $l_{A-B} = 80$ mm, toleranced element between datums.

h_i mm	bs_i μm	u_{p_i} μm	U_{2_i} μm	U_{SA1_i} μm ($b_1 = 0.577$)	U_{SA2_i} μm ($b_2 = 0.459$)	$\chi^2_1(b_1 = 0.577)$	$\chi^2_2(b_2 = 0.459)$
5	3.09	2.28	7.93	9.26	7.36	14.68	23.23
10	2.66	1.03	6.05	9.31	7.40	8.44	13.35
15	3.02	1.14	6.75	9.40	7.47	10.32	16.33
20	2.62	1.38	6.25	9.52	7.57	8.61	13.62
25	3.06	1.21	6.88	9.68	7.69	10.11	16.00
30	2.50	1.42	6.08	9.87	7.84	7.59	12.01
35	2.70	1.83	6.83	10.08	8.02	9.17	14.50
40	4.65	3.16	11.42	10.33	8.21	24.46	38.70
35	4.26	3.63	11.37	10.08	8.02	25.44	40.25
30	3.40	3.38	9.80	9.87	7.84	19.72	31.21
25	3.70	1.94	8.59	9.68	7.69	15.74	24.91
20	4.09	2.20	9.50	9.52	7.57	19.91	31.50
15	3.77	2.06	8.82	9.40	7.47	17.61	27.86
10	3.03	1.72	7.24	9.31	7.40	12.11	19.16
5	3.08	1.46	7.11	9.26	7.36	11.80	18.66

method. The chi-square test value is calculated by the formula.

$$\chi^2 = \frac{n\sigma^2}{\sigma_{SA}^2} \tag{18}$$

where σ and σ_{SA} are the standard uncertainties evaluated experimentally and using the SA method, respectively, and n is the size of the sample (20). Critical values χ^2_{cr1} and χ^2_{cr2} used as the limits in the tests are 2.5 % and 97.5 % quantiles, respectively, of a chi-square distribution with 19 degrees of freedom. The main characteristics of the test are summarized in Table 5.

The chi-square values obtained from the analysis will be highlighted in three colours (Table 6).

5.4. Results for the diameter

The measurements of all the 17 sections of the cylinder were individually considered and their diameters were evaluated. The comparison of the uncertainties evaluated experimentally (either U_1 or U_2) and using the SA method (U_{SA}) is reported in Fig. 9. The uncertainty budget for b_1 is in Table 2.

Uncertainty values U_1 and U_2 , calculated according to the formulae (14) (upper row) and (15) (lower row), are marked with dots on the diagram. The U_{SA} uncertainty values are marked with vertical lines: on the right U_{SA1} , and on the left U_{SA2} . It can be seen from the graph that the U_{SA1} value shows better agreement with the results of the experiment. Statistically unambiguous results can be obtained only after applying the chi-square test.

The experimentally obtained uncertainty values U_1 and U_2 and the chi-square test values for comparison with the uncertainties U_{SA} calculated using the SA method are shown in Table 7.

The chi-square test fully confirms the consistency of the results obtained by the SA method assuming uniform distribution ($U_{SA1} = 7.49$),

both compared with U_1 and U_2 . When included the results of the reverification test ($U_{SA2} = 5.95$) the SA method gives slightly worse results: for 17 comparisons 4 negative results were obtained compared to U_1 , and 1 negative results compared to U_2 . In the all 5 cases, the results obtained using the SA method are considered to be underestimated by the chi-square test. In general, the results of the validation tests for the circle diameter can be deemed very satisfactory.

Looking at the bs values in the subsequent sections of the cylinder, it cannot be ruled out that the cause is the conicity of the cylinder (the method of calibrating the cylinder diameter is not known - the calibration certificate contained one value).

5.5. Results for coaxiality

In Fig. 10 for all the lengths of the datum l_A and common datum A-B for all the distances of the toleranced element from the datum, the expanded uncertainties determined experimentally and the uncertainties evaluated using the SA method are shown. The solid lines refer to the uncertainties evaluated using the SA method. The upper one is the U_{SA1} , the lower - U_{SA2} values. The dots represent U_1 , U_2 , U_{4W} i U_{4R} values. of the experimentally obtained uncertainties. The uncertainty budget for one of those points is given in Table 3.

Please note that the successive graphs use clearly different magnifications. The last graph summarizes the uncertainty U_{SA1} . The curves illustrate the uncertainties for the successive datum lengths: the highest curve (blue) is for $l_A = 10$ mm, the successive datums with their lengths increased up to $l_A = 35$ mm for the lowest, penultimate datum (green). The lowest (blue) applies to the common datum A-B.

A important characteristic of the performed tests is the fact that a very wide range of measurement uncertainty, from 8 to 66 μm, was obtained. The graphs show that the use of different formulae for the experimental determination of the measurement uncertainty gives quite clear differences in the results. Similarly, including, or not taking into account the reverification test results when calculating the uncertainty using the SA method, gives a significant difference in the obtained results.

The graphs show a good correlation between the results calculated using the SA method and the results obtained by the experiment according to [9]. This confirms the particular usefulness of the cylindrical square in validating different methods for evaluating the uncertainty of coordinate measurements.

Let us also note that the formula for U_2 gives the highest values of the uncertainty determined experimentally, whereas the formula for U_{4R} gives the lowest ones. The range of uncertainty assessments is also considerable, particularly in comparison with the difference in the results obtained through the SA method.

A comparison of the measurement uncertainty calculated using the SA method with the results obtained experimentally according to [9] may also be presented differently. In Fig. 11, the resulting error values are compared against the lines representing the calculated measurement uncertainty. An example graph refers to coaxiality relative to a common datum. According to the definition of expanded measurement uncertainty, it is expected that approximately 95% of the error values should

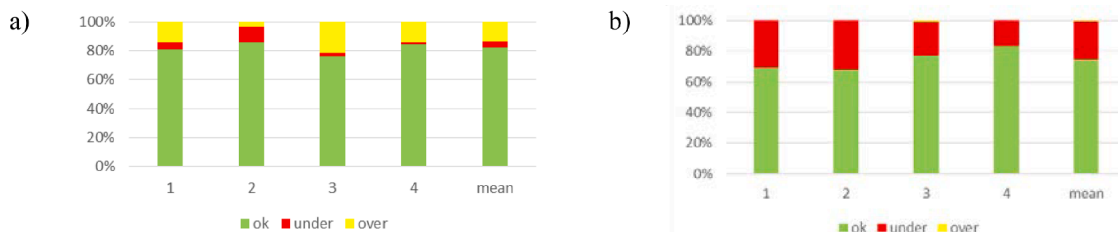


Fig. 12. Results of the chi-square test for: a) U_{SA1} , b) U_{SA2} . The first 4 bars correspond successively to the experimental uncertainties U_1 , U_2 , U_{4W} and U_{4R} , the fifth bar contains the averaged values.

be less than the expanded measurement uncertainty. When looking at the results obtained globally, this condition can be considered to be met even for the uncertainties U_{SA2} , because only 14 from 300 error values exceed the uncertainty values, which represents 4.8 % of all values. For the remaining cases analysed, the lengths of the datum ranging from 10 mm to 35 mm, the results obtained were following, respectively (in %): 0, 5.8, 5.0, 8.2, 8.5 and 9.4. Similar calculations for U_{SA1} give the following results: 1.7, 0, 1.2, 2.1, 2.3, 3.5 and 5.0 % (the value of 5 % is not exceeded in any case).

An informal analysis of the test results has been discussed so far. The chi-square test for equality of variances was used for the formal assessment. Table 8 provides a comparison of the uncertainty U_2 with two cases of uncertainty U_{SA} calculated using the SA method.

The positive test results are shown in green (no grounds for rejection of a hypothesis of variance equality). The instances of significant overestimation of the uncertainty are highlighted in yellow and the significant underestimation in red.

This analysis was performed for all the 17 coaxiality cases (84 in total) and all the 4 methods of determining experimental uncertainty. The results of this analysis are summarized in Fig. 12.

It would be good to examine the components of experimental uncertainty in more detail. Table 8 shows (and it is similar for other cases) that the largest component of experimental uncertainty is bias b_s .

There are 84 results in total. There are more positive results for U_{SA1} . Among the negative results, mainly are the underestimations, that are acceptable in the uncertainty analyses. The best results were obtained when experimental uncertainty was determined using the Rayleigh distribution (U_{4R}). The presented results confirm that adopting the uniform distribution for distance measurement errors is correct. The expected benefit of considering the current CMM accuracy has not been proven. In this regard, it is advisable to repeat the tests on the CMM, the actual errors of which are clearly lower than the permissible ones.

6. Conclusions

The validation of the method for determining the uncertainty (SA method) developed at ATH was carried out on one CMM. An accessible and easy to calibrate artifact - cylindrical square was used for validation. The experiment was designed in such a way that a large range of measurement uncertainty is obtained (in the above-mentioned example, for various coaxiality measurement strategies, measurement uncertainties ranging from 8 μm to 66 μm were obtained). The obtained results confirm the correctness of the SA method.

The experiment is easy to perform (repeat) on any CMM, it only requires measurements of the diameter and coordinates of the centre of 17 circles (measurements should be repeated 20 times at one- or two-day intervals) - the processing of the results can be performed in a developed and available on request spreadsheet.

Most of the characteristics appearing in construction drawings are geometric deviations, which assume only non-negative values. The obtained results indicate that the Rayleigh distribution is well suited for the development of the results of the experimental determination of the measurement uncertainty of such characteristics.

The results obtained confirmed that the cylindrical square is ideal for the validation of any UES. The measurement itself is short because it consists solely of measuring 17 circles - the rest of the calculations can be performed in a pre-designed spreadsheet made available by authors. A particular advantage is the large range of uncertainties obtained for the different variants of datum lengths and toleranced element-to-datum distances.

According to ISO 15530-3 recommendations, the cylindrical square measurement described should be repeated 20 times at a minimum of one-, two-day intervals, but once fewer repetitions have been performed, e.g. 10, reliable information can be obtained.

The article compares 4 different methods of developing the results of the experiment: formulae (15), (16) and (18), and in the case of formula

(18), 2 different Weibull and Rayleigh probability distributions. The performed tests show that in the case of characteristics with both positive and negative values (e.g. diameter deviations), the best results are obtained by using the formula (16), and in the case of characteristics with non-negative values (geometric deviations) - by using the formula (18) and the Rayleigh distribution.

With regard to the SA method, the article analyses the advisability of taking into account the information contained in the CMM calibration results (in comparison with the a priori adopted uniform distribution of errors). The obtained results do not confirm this purposefulness. It should be noted, however, that the observed CMM error distribution differed only slightly from the uniform distribution and, in addition, was asymmetric.

As a side note, it is worth mentioning that for some characteristics it is possible to derive general formulae for the measurement uncertainty for the SA method. The article provides such formulae for the measurement uncertainty of concentricity and circle diameter.

The authors are convinced that the positive result of validation for the circle diameter and the coaxiality can be generalized to all characteristics for which the measurement uncertainty has been evaluated using the SA method described.

The fact that in majority of industrial measurements it is not possible to apply bias correction, as well as the fact that mainly geometrical deviations (only non-negative deviations) are measured in industry, should be taken into account when amending the ISO 15530-3 standard.

CRediT authorship contribution statement

Mirosław Wojtyła: Investigation, Resources, Formal analysis, Writing - original draft, Writing - review & editing. **Paweł Rosner:** Investigation, Resources, Formal analysis, Writing - original draft. **Wojciech Płowucha:** Methodology, Supervision, Formal analysis, Writing - review & editing. **Alistair B. Forbes:** Data curation. **Enrico Savio:** Data curation. **Alessandro Balsamo:** Funding acquisition, Project administration.

Declaration of Competing Interest

The authors declare that they have no known competing financial interests or personal relationships that could have appeared to influence the work reported in this paper.

Acknowledgments

The presented work is part of the EMPIR EURAMET-founded joint research project no. 17NRM03 "Standards for the evaluation of the uncertainty of coordinate measurements in industry EUCoM" coordinated by Alessandro Balsamo, INRIM.

References

- [1] JCGM 100, Evaluation of measurement data. Guide to the expression of uncertainty in measurement, 2008.
- [2] ISO/IEC Guide 98-4, Uncertainty of measurement. Role of measurement uncertainty in conformity assessments, 2012.
- [3] ISO 14253-1, Geometrical product specifications (GPS). Inspection by measurement of workpieces and measuring equipment - Part 1: Decision rules for verifying conformity or nonconformity with specification, 2017.
- [4] IATF 16949, Quality management systems requirements for automotive production and relevant service part organizations, 2016.
- [5] R.G.G. Wilhelm, R. Hocken, H. Schwenke, Task Specific Uncertainty in Coordinate Measurement, CIRP Annals - Manufacturing Technology. 50 (2001) 553-563, [https://doi.org/10.1016/S0007-8506\(07\)62995-3](https://doi.org/10.1016/S0007-8506(07)62995-3).
- [6] ISO 1101 Geometrical product specifications (GPS) - Geometrical tolerancing - Tolerances of form, orientation, location and run-out, 2017.
- [7] Z. Humienny, State of art in standardization in the geometrical product specification area - a decade later, CIRP Journal of Manufacturing Science and Technology 33 (2021) 42-51, <https://doi.org/10.1016/j.cirpj.2021.02.009>.
- [8] EA-4/02 M, Expression of the Uncertainty of Measurement in Calibration. European co-operation for Accreditation, 2013.

- [9] ISO 15530-3, Geometrical product specifications (GPS) - Coordinate measuring machines (CMM): Technique for determining the uncertainty of measurement - Part 3: Use of calibrated workpieces or measurement standards, 2011.
- [10] ISO/TS 15530-1, Geometrical product specifications (GPS) - Coordinate measuring machines (CMM): Technique for determining the uncertainty of measurement - Part 1: Overview and metrological characteristics, 2013.
- [11] ISO/TS 15530-4, Geometrical Product Specifications (GPS) - Coordinate measuring machines (CMM): Technique for determining the uncertainty of measurement - Part 4: Evaluating task-specific measurement uncertainty using simulation, 2008.
- [12] VDI/VDE 2617, Part 11, Accuracy of coordinate measuring machines. Characteristics and their checking. Determination of the uncertainty of measurement for coordinate measuring machines using uncertainty budgets, 2011.
- [13] E. Trapet, M. Franke, F. Härtig, H. Schwenke, F. Wäldele, M. Cox, A. Forbes, F. Delbressine, P. Schellekens, M. Trenk, H. Meyer, G. Moritz, T.h. Guth, N. Wanner, Traceability of Coordinate Measurements According to the Method of the Virtual Measuring Machine, Part 2 of the Final Report Project MAT1-CT94-0076, Braunschweig (1999).
- [14] M. Franke, T. Kistner, T. Hausotte, D. Heisselmann, C. Schwehn, K. Wendt, Determination of the measurement uncertainty of coordinate measuring systems, *tm - Technisches Messen*. 84 (2017) 325–335. doi:10.1515/teme-2017-0016.
- [15] Y. Cheng, Z. Wang, X. Chen, Y. Li, H. Li, H. Li, H. Wang, Evaluation and Optimization of Task-oriented Measurement Uncertainty for Coordinate Measuring Machines Based on Geometrical Product Specifications, *Applied Sciences*. 9 (2018) 6, <https://doi.org/10.3390/app9010006>.
- [16] A. Gaška, W. Harmatys, P. Gaška, M. Gruzka, K. Gromczak, K. Ostrowska, Virtual CMM-based model for uncertainty estimation of coordinate measurements performed in industrial conditions, *Measurement* 98 (2017) 361–371, <https://doi.org/10.1016/j.measurement.2016.12.027>.
- [17] A. Jalid, S. Hariri, N.E. Laghzale, Influence of sample size on flatness estimation and uncertainty in three-dimensional measurement, *Int. J. Metrol. Qual. Eng.* 6 (2015) 102, <https://doi.org/10.1051/ijmqe/2015002>.
- [18] O. Sato, S. Osawa, Y. Kondo, M. Komori, T. Takatsuji, Calibration and uncertainty evaluation of single pitch deviation by multiple-measurement technique, *Precision Engineering* 34 (2010) 156–163, <https://doi.org/10.1016/j.precisioneng.2009.05.009>.
- [19] Evaluating Uncertainty in Coordinate Measurements. <https://eucom-empir.eu/>, 2021 (accessed on 18.04.2021).
- [20] W. Płowucha, Point-straight line distance as model for uncertainty evaluation of coordinate measurement, *Measurement*. 135 (2019) 83–95, <https://doi.org/10.1016/j.measurement.2018.11.008>.
- [21] W. Płowucha, Point-plane distance as model for uncertainty evaluation of coordinate measurement, *Metrol. Meas. Syst.* 27 (4) (2020) 625–639. <https://doi.org/10.24425/mms.2020.134843>.
- [22] ISO 17450-1, Geometrical product specifications (GPS) - General concepts - Part 1: Model for geometrical specification and verification, 2011.
- [23] ISO 10360-2, Geometrical product specifications (GPS) - Acceptance and reverification tests for coordinate measuring machines (CMM) - Part 2: CMMs used for measuring linear dimensions, 2009.
- [24] ISO 14253-2, Geometrical product specifications (GPS) - Inspection by measurement of workpieces and measuring equipment - Part 2: Guidance for the estimation of uncertainty in GPS measurement, in calibration of measuring equipment and in product verification, 2011.
- [25] W. Płowucha, Evaluation of coordinate measurement uncertainty by sensitivity analysis – theoretical background, *Mechanik* 91 (11) (2018) 953–956. <https://doi.org/10.17814/mechanik.2018.11.168>.
- [26] ISO 3534-1, Statistics - Vocabulary and symbols - Part 1: General statistical terms and terms used in probability, 2006.
- [27] ISO/TS 15530-3, Geometrical Product Specifications (GPS) - Coordinate measuring machines (CMM): Technique for determining the uncertainty of measurement - Part 3: Use of calibrated workpieces or standards (old edition of [9]), 2004.
- [28] F. Härtig, M. Krystek Correct treatment of systematic errors in the evaluation of measurement uncertainty, http://www.ets.ifmo.ru/tomasov/konferenc/AutoPlay/Docs/Volume%201/1_04.pdf.